THE FLOW AND HEAD DISTRIBUTION WITHIN THE VOLUTE OF A CENTRIFUGAL PUMP IN COMPARISON WITH THE CHARACTERISTICS OF THE IMPELLER WITHOUT CASING

Peter Hergt, Stephan Meschkat and Bernd Stoffel
Chair of Turbomachinery and Fluid Power, Darmstadt University
67059 Ludwigshafen, Germany
meschkat@tfa.maschinenbau.tu-darmstadt.de

Abstract. Measurements of the unsteady velocity, pressure and flow angle have been carried out at the impeller outlet of a centrifugal pump with and without volute casing at 5 operating points using the hotwire technology and a fast response single hole cylindrical probe. The test fluid was air. While the velocities and pressures depend only on the axial coordinate and are rotationally symmetrical, if there is no casing around the impeller, the influence of the volute on the circumferential distribution of these quantities increases with the deviation of the operating point from the design point. With respect to the local throughflow distribution, this influence is much more pronounced in comparison to the pressure distribution.

Keywords: spiral casing pump, rotor stator interaction, experimental investigation

Nomenclature

b	$[mm]$	width of the vaneless radial diffuser, inlet width of the volute ($42\,mm$)
c_m	$[m/s]$	meridional velocity at, r_M
r_M	$[mm]$	radial position of the measuring section ($208.5\,mm$)
u_2	$[m/s]$	peripheral velocity at the impeller outlet
x	$[mm]$	axial distance from the front shroud at, r_M
H	$[m]$	total head
Q	$[m^3/s]$	flow rate
Q_{des}	$[m^3/s]$	flow rate at design point
ε	$[\circ]$	circumferential angle from the tongue in the sense of rotation
φ	$[-]$	flow coefficient, c_m/u_2
φ_{des}	$[-]$	flow coefficient at design point
$\bar{\varphi}$	$[-]$	local mean value of $\varphi = \int_0^1 \varphi\, d\left(\frac{x}{b}\right)$
$\bar{\bar{\varphi}}$	$[-]$	local mean value of $\varphi = \frac{1}{2\pi}\int_0^{2\pi} \bar{\varphi}\, d\varepsilon$
ψ	$[-]$	pressure coefficient, $\frac{2gH}{u_2^2}$

1. Introduction

Single stage centrifugal pumps are mostly designed and produced with a volute casing. It is well known that – in this case – the flow at the impeller outlet can only be nearly independent of the circumferential position in the volute if the volute geometry is well designed and the pump is operated at its design point. For off-design operation of volute casing pumps, the volute casing geometry does not 'fit' the outflow from the impeller. This leads to a non-uniform distribution of (time averaged) pressure and velocity along the circumference of the volute.

Different approaches exist for modelling this type of rotor-stator-interactions in turbomachines (mixing plane, frozen rotor, transient), see e.g. [2, 5]. To compare the capabilities of the respective modellings in taking into account and describing important features of off-design flow in volute casing pumps, detailed flow field measurements and evaluations are needed.

A research project was carried out at the Laboratory for Turbomachinery and Fluid Power of the Darmstadt University of Technology which aimed at gaining more insight into the aspects of rotor-stator interactions in volute casing pumps and – additionally – creating a data basis for the validation of CFD simulations. Likewise experimental investigations on rotor stator interactions can be found in [1, 2, 4-8].

2. Test rig

The test rig and its instrumentation which was described in more detail in [4] are suited for measurements of transient velocity and pressure distribution for different circumferential positions inside the volute near the impeller outlet. For this purpose and to enable a continuous variation of the measuring positions along the whole circumference of the volute, the volute casing of the test pump can be turned by an electrical motor around the pump axis while the mechanism for traversing the probes is mounted to a fixed inner part of the casing and remains at a constant location. Table 1 shows the technical data of the pump.

Table 2. Technical specifications

Impeller outlet diameter	:	$405\,mm$
Impeller outlet width	:	$38\,mm$
Impeller inlet diameter	:	$240\,mm$
Blade number	:	7
Outlet angle, shroud	:	$25°$
Outlet angle, hub	:	$29°$
Specific speed	:	$35\,min^{-1}$
Rotational speed	:	$3000\,min^{-1}$
Design flow rate	:	$1380\,m^3/h$

As can be seen in Figure 1, the inner part of the casing is mounted on two vertical uprights on the front side and rear side while the turnable volute casing is supported on the inner parts (see Figure 2) by ball bearings. For the sealing between both parts of the casing, sheets of felt are used.
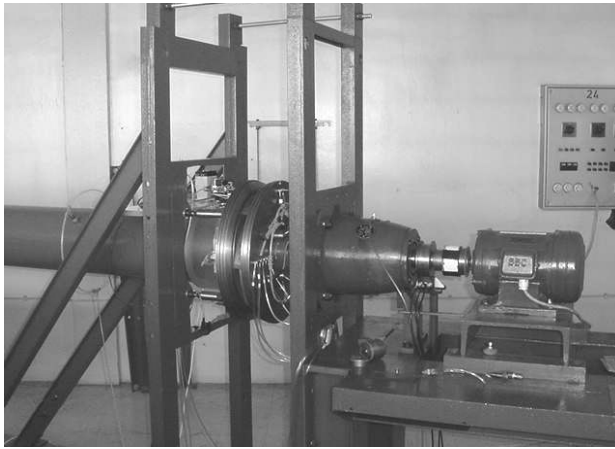

Figure 1. Test rig configuration without volute

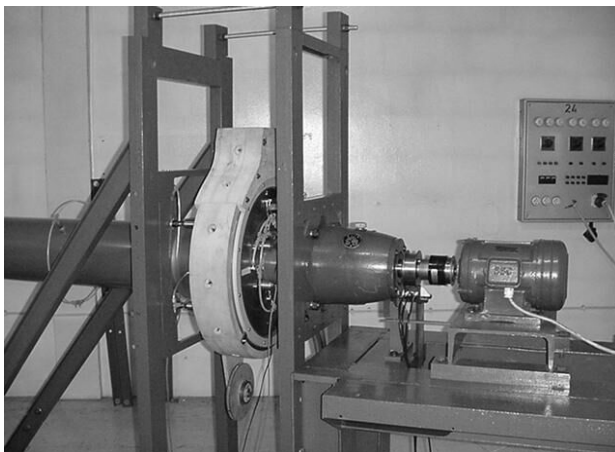The configuration with mounted volute is shown in Figure 2.

Figure 2. Test rig with mounted volute

In the case of the test rig configuration without the volute part of the casing (Figure 1), flow measurements are possible for free impeller discharge where the pressure at the impeller outlet is constant (= atmospheric pressure) along the impeller outlet.

The analysis of flow was performed by the use of hotwire anemometry and a fast response single hole cylindrical probe [4] which were located $6\,mm$ radially outward of the impeller outlet. Using this single hole cylindrical probe with an integrated high frequency response pressure transducer gives information on the unsteady static and total pressure of the flow from which also the flow velocity can be calculated. But from the experience gained, more reliable information on the unsteady velocity and flow angle is found from a single-wired hotwire probe.

Both probes are traversed across the width of the impeller outlet (see Figure 3). As the probes are turned stepwise around their longitudinal axis at each axial position while the flow direction is nearly perpendicular to the longitudinal axis, the flow angle can be determined by calculating the position of the maximum of measurement data for all time steps (as an ensembled average value in dependence of the angular impeller position and as a time-averaged value, as well).
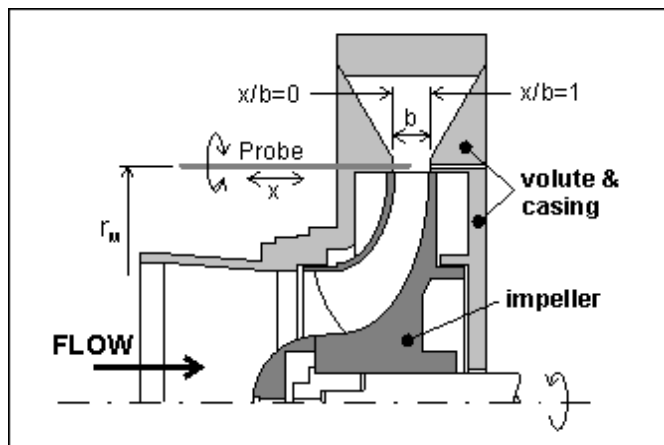

Figure 3. Meridional contour and position of probe

The circumferential distribution of pressure on the surface of the single hole cylindrical probe is detected through a $0.3\,mm$ diameter hole. A calibration for different constant velocities allows one to find the exact maximum pressure position and to determine a circumferential position on the cylinder surface where the measured pressure equals the local static pressure in the flow. The angle of the position where the measured pressure indicates the static pressure of the flow remains constant for a wide range of velocities as described in Schlichting [3]. Because transient effects in unsteady flow influence the circumferential pressure distribution on the probe surface and thus especially the right position where the surface pressure equals the local static pressure of the flow, the determination of the flow direction and magnitude of velocity is done additionally by the hotwire technique.

3. Results and discussion

3.1. **Impeller without casing, throughflow.** The distribution of the throughflow component φ is plotted versus the dimensionless axial coordinate in Figure 4 for various values of the normalized flow rate Q/Q_{des}. The character of the curves is well known from other publications and shows that the main throughflow takes place near the rear shroud.
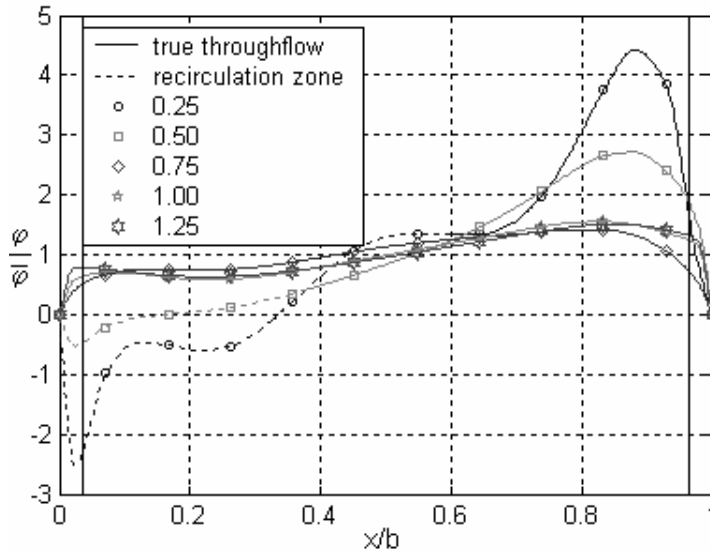

Figure 4. Distribution of the meridional velocity, without casing

At strongly reduced flow rates ($Q/Q_{des} = 0.50$ and 0.25), backflow occurs at the measuring location near the front shroud. Because of the flow recirculation inside and outside the impeller, part of the outflow from the impeller serves to compensate the backflow in the balance of mass flow. Therefore, only the remaining part of the outflow is representative for the mass transport through the pump and is called 'true throughflow'. In Figure 4, the broken part of the curves indicates the width of the recirculation zone within which the part of the outflow only compensates the backflow. All distributions are rotationally symmetrical.

3.2. **Impeller without casing, head.** The distribution of the local head is shown in Figure 5. While the head is nearly independent of the axial coordinate at high flow rates, higher heads are measured near the rear shroud at low flow rates. This is somewhat surprising because this is also the area with the higher meridional velocities, i.e. local throughflow (see Figure 4).
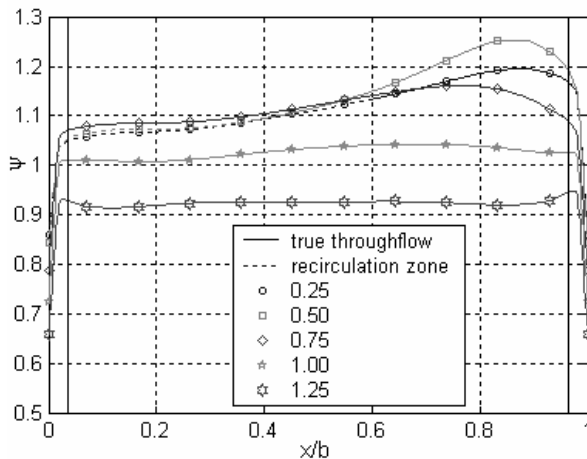
Figure 5. Distribution of local head, without casing

3.3. **Throughflow distribution at the volute inlet.** The meridional component characterising the local throughflow in the measuring section (that is now the volute inlet) is shown for 5 values of the normalized flow rate in Figure 6.

The broken curves on the diagrams for 75%, 50% and 25% of the design flow rate represent the limit of the true throughflow area. The remaining area characterises the recirculation zone with a negative and the corresponding positive flow rate.Whereas the high meridional velocities are still found near the rear shroud, the circumferential distribution becomes the more irregular the more the flow rate deviates from the design value. It can clearly be observed from the distributions that at part load flow rates, only part of the volute width and circumference contribute to the true throughflow while outside this area backflow and forward flow compensate each other and no net mass flow results. The borderline between the backflow area and the forward flow area can be identified from the isocontour having the value 0 of the dimensionless meridional component.

At 125% of the design flow rate, the highest throughflow component has been measured approximately 30° upstream of the tongue, which means that the local flow rate increases along the circumference as is found also by theoretical considerations.

Contrary to this, the local flow rate decreases along the circumference if the pump is operated at low flow rates which is also in correspondence with the theory.

At 25% of design flow rate, less than half of the volute inlet cross-section contributes to the throughflow. The rest consists of a strong recirculation especially just upstream of the tongue where no true throughflow exists. Referring to the impeller frame of reference, it becomes evident that blade channels passing through this area of the volute do not contribute to the net impeller mass flow and are exposed to strong backflow once per each impeller revolution.
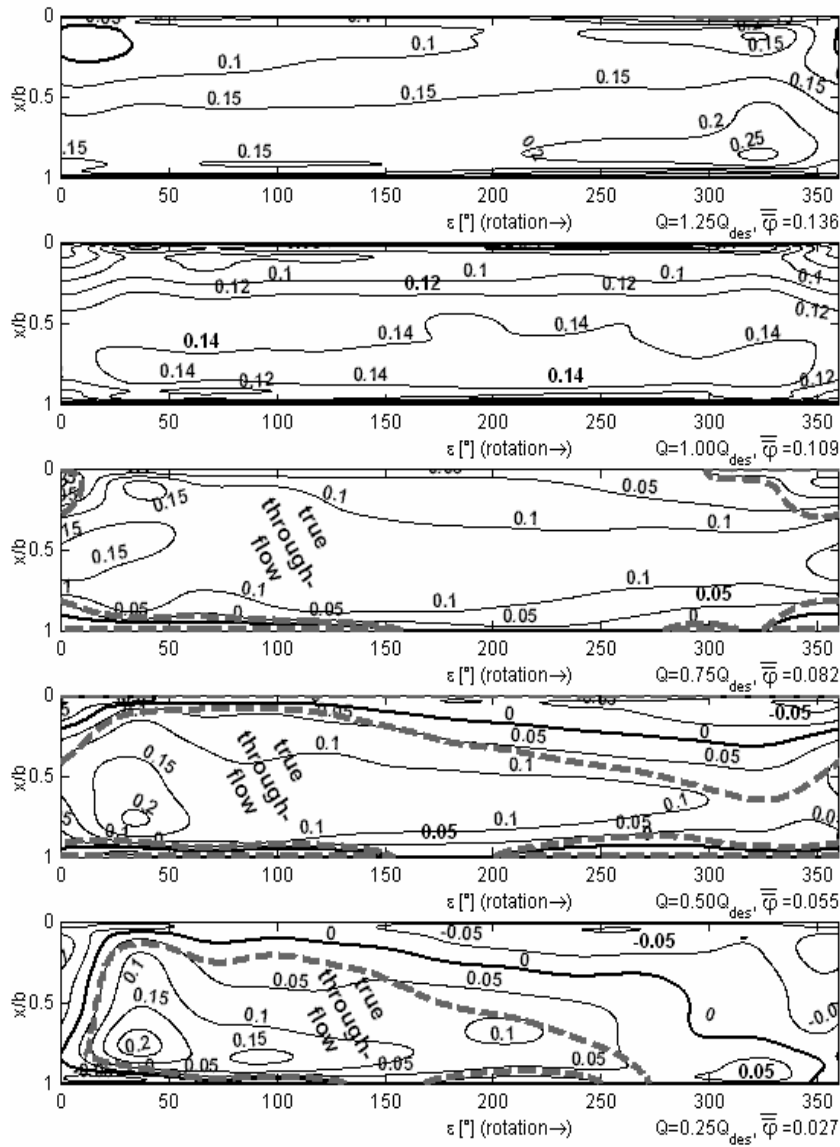
Figure 6. Distribution of meridional component at the volute inlet

The curves in Figure 7 underline the findings for 50% flow rate and some selected circumferential positions.

The local $\bar{\varphi}$-values related to the true throughflow coefficient $\bar{\bar{\varphi}}$ are plotted in Figure 8 versus the angular position.
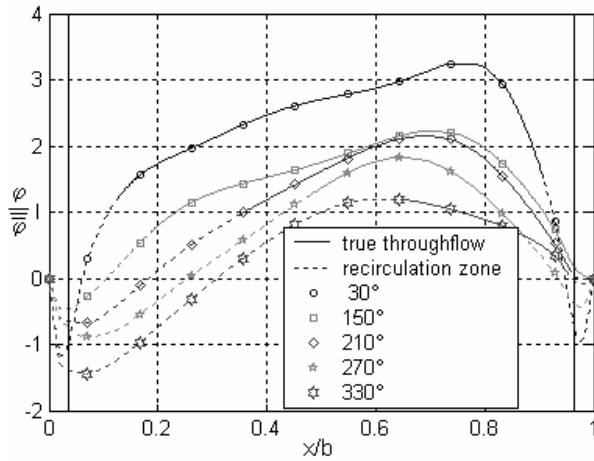
Figure 7. $\varphi/\bar{\bar{\varphi}}$ for different circumferential positions. $\varphi = 0.5 \cdot \varphi_{des}$
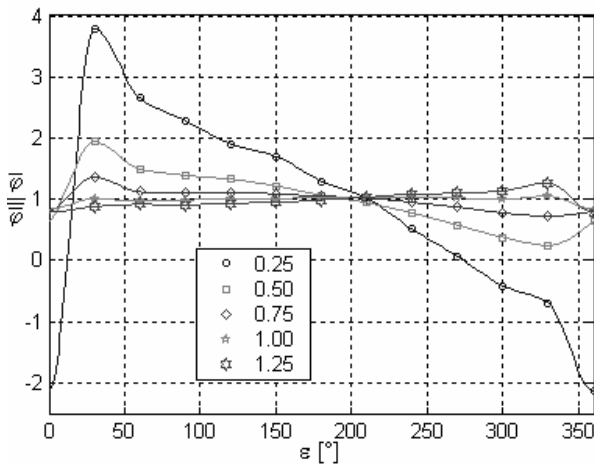

Figure 8. Local $\bar{\varphi}$-values depending on the angular position

Two facts are striking in the context:

i) $\bar{\varphi} = \bar{\bar{\varphi}}$ at approximately 205° for all flowrates.

ii) $\bar{\varphi}$ is approximately independent of the flow rate at ca. 30° downstream of the tongue ($3.8 \times 0.25 \approx 1.95 \times 0.5...$ etc.)

This seems to be an interesting feature of the impeller-volute interaction but cannot yet be explained at present.
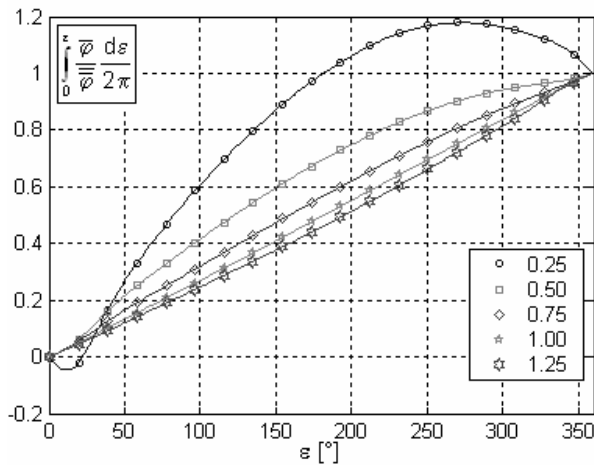
Figure 9. Flow rate integrated along the circumference

Integrating the local flow rates along the circumference leads to Figure 9.

As it could be expected already from Figure 6 there is a linear dependence between the flow rate and the angular position at $\varphi = \varphi_{des}$, while the local flow rate increases up to $1.2 \times \bar{\bar{\varphi}}\,(\epsilon \approx 270°)$ and falls down to $1.0 \times \bar{\bar{\varphi}}$ in the following sections due to the strong backflow in this area (see Figure 6).

3.4. **Head distribution at the volute inlet.** In addition to the throughflow distribution of Figure 6, the distribution of head is shown in Figure 10. Again, the broken lines characterize the true throughflow areas.

In comparison to the distribution of the meridional velocity, the distribution of head is more regular along the width of the measurement section for overload and design point. For part load, the shape along the width deviates from a flat distribution to a distribution with increased head near the rear shroud as this can also be found for the head distribution of the impeller without casing in Figure 5.

As expected, the circumferential distribution becomes more irregular with increasing deviation from the design flow rate. This could at least partially be caused by the variation of the circumferential velocity components. The lowest pressure coefficients have been measured in the backflow zones ($\varphi < 0$) where a part of the energy has been lost through wall friction and mixing losses.

A detailed explanation of the relations between flow and head distribution is rather difficult due to the lack of information about what is caused by separation and recirculation within the impeller on the one side and within the volute only on the other side.
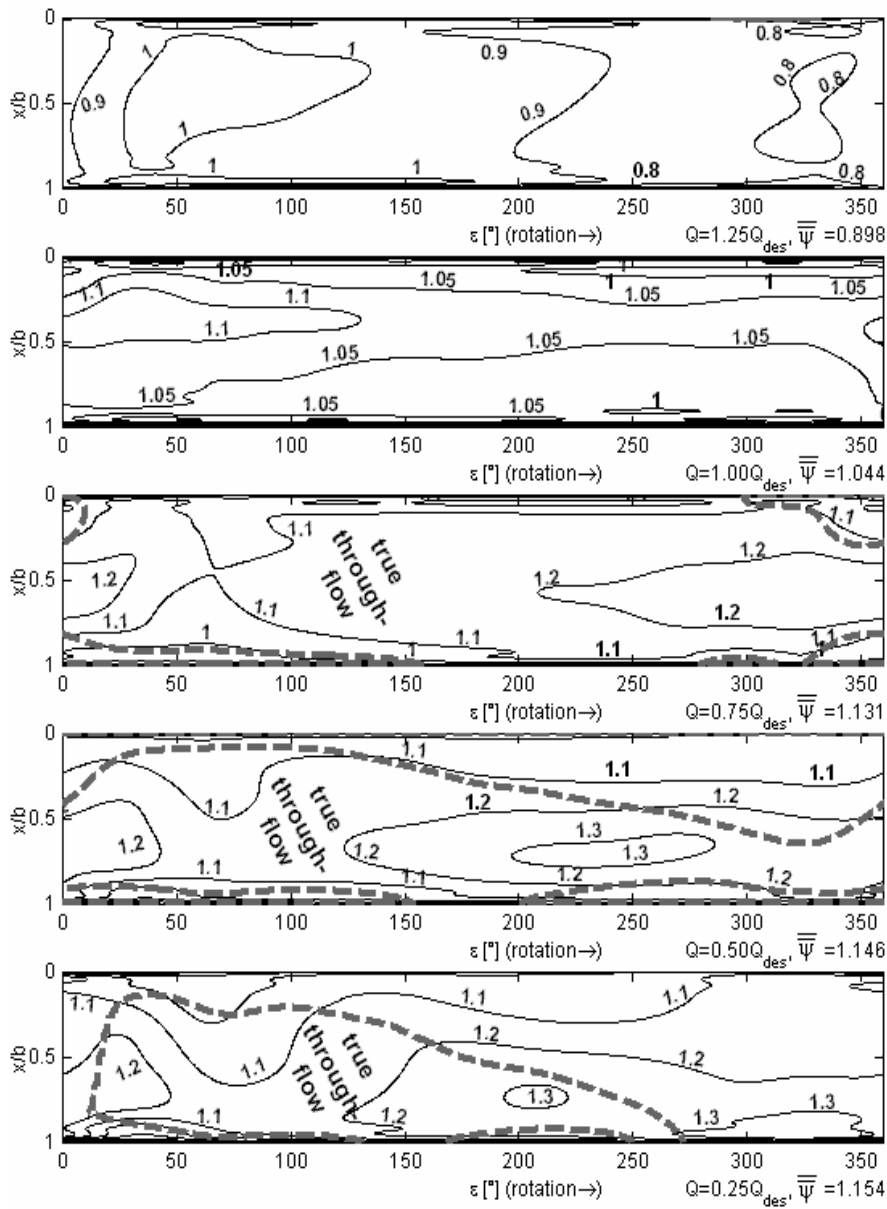
Figure 10. Distribution of local head at the volute inlet

To get this information, measurements within the impeller would be necessary in addition.

4. Summary

Distributions of flow and head at the impeller outlet in a centrifugal pump with volute casing were shown. Some typical distributions for these kinds of pumps were explained and discussed. Most of the results are strictly related to theory. Thus the findings and the qualitative shape of the illustrated graphs and distributions can serve as an orientation for computational fluid dynamics and may encourage researchers to do similar analysis in the frame of postprocessing such calculations.

REFERENCES

1. FLÖRKEMEIER K.H.: *Experimentelle Untersuchungen zur Optimierung von Spiral-gehäusepumpen mit tangentialem und radialem Druckstutzen*, PhD-Thesis, TU Braunschweig, 1977.

2. FRITZ, J.: *Strömungswechselwirkungen in hydraulischen Maschinen*, PhD-Thesis, TU München, 1999.

3. SCHLICHTING, H. AND GERSTEN, K.: *Boundary Layer Theory*, Springer-Verlag, Berlin, New York, 1999.

4. STOFFEL, B. AND MESCHKAT, S.: The local specific head at different circumferential positions in a volute casing centrifugal pump in comparison to the characteristic curve of the single rotor, *Proceedings of the Hydraulic Machinery and Systems 21st IAHR Symposium*, Lausanne, 2002.

5. TREUTZ, G.: *Numerische Simulation der instatonären Strömung in einer Kreiselpumpe*, PhD-Thesis, TU Darmstadt, 2002.

6. WEISS, K.: *Experimentelle Untersuchungen zur Teillastströmung bei Kreiselpumpen*, PhD-Thesis, U Darmstadt, 1995.

7. UBALDI, M.: An experimental investigation of stator induced unsteadiness on centrifugal impeller outflow. *Journal of Turbomachinery*, **118**, (1996), 41–54.

8. UBALDI, M.: Relative flow and turbulence measurements downstream of a backward centrifugal impeller. *Journal of Turbomachinery*, **113**, (1993), 543–551.